












Thermal plasticity of coral reef symbionts is linked to major alterations in their lipidome composition

Marina T. Botana ^{1*,a} Adriano B. Chaves-Filho ² Alex Inague ² Arthur Z. Güth ¹
Flavia Saldanha-Corrêa ¹ Marius N. Müller ³ Paulo Y. G. Sumida ¹ Sayuri Miyamoto ²
Matthias Y. Kellermann ⁴ Raymond C. Valentine ⁵ Marcos Y. Yoshinaga ^{2*}

¹Instituto Oceanográfico, Universidade de São Paulo, São Paulo, São Paulo

²Instituto de Química, Universidade de São Paulo, São Paulo, São Paulo

³Departamento de Oceanografia, Universidade Federal de Pernambuco, Recife, Brazil

⁴Institute for Chemistry and Biology of the Marine Environment (ICBM), Carl-von-Ossietzky University, Oldenburg, Germany

⁵University of California, Davis, California

Abstract

Coral bleaching caused by ocean warming is leading to worldwide coral decline. The physiological processes underlying this ecological event are still incompletely understood, although previous research has suggested oxidative stress as major player in the impairment of symbiont thylakoid membranes and in symbiosis breakdown. Lipids are interesting targets of investigation, given their susceptibility to thermal and oxidative stresses. Here, an untargeted lipidomic approach was employed to examine changes in lipidome and pigments of three coral reef symbionts (Symbiodiniaceae) after a heat shock in *in vitro* experiments. The acute thermal stress induced species-specific changes in lipidome and pigments compositions of both heat sensitive and tolerant symbionts. Heat sensitivity was characterized by a steep and steady decline in cell densities over time (4 and 240 h after heat shock). At the membrane level, heat sensitive symbiont displayed a quantitative decrease in glycolipids linked to polyunsaturated fatty acids, followed by enrichment in oxidized lipids and sphingolipids. Despite showing distinct adaptations, the two heat tolerant symbionts were characterized by the preservation of membrane lipids after heat shock, particularly glycolipids. This finding suggests the action of powerful antioxidant systems, preventing the escalation of oxidized lipids concentration in thylakoid membranes under thermal stress. Although limited by the examination of free-living symbionts, our study provides a solid baseline for the investigation of lipidome and pigments alterations of Symbiodiniaceae in response to heat stress. Novel potential lipid biomarkers linked to thermal stress are suggested. In particular, oxidized lipids—which are implicated in coral symbiosis establishment and breakdown—appear as attractive targets for further research.

*Correspondence: marina.tonettibotana@vuw.ac.nz; marcosyukio@gmail.com

This is an open access article under the terms of the [Creative Commons Attribution](#) License, which permits use, distribution and reproduction in any medium, provided the original work is properly cited.

Additional Supporting Information may be found in the online version of this article.

^aPresent address: School of Biological Sciences, Victoria University of Wellington, New Zealand

Author contribution statement: M.T.B. experiment, lipidomics, data analysis and manuscript writing; A.B.C.F. analytical design, lipidomics and oxylipidomics; A.I. lipidomics; A.Z.G. data analysis and manuscript writing; F.S.C. study design; M.N.M. study design and manuscript writing; P.Y.G.S. study design and project funding; S.M. analytical design, lipidomics and oxylipidomics; M.Y.K. lipidomics and study design; R.C. V. study design; M.Y.Y. lipidomics, oxylipidomics and manuscript writing. All authors provided substantial comments on the manuscript.

The lipid composition of energy-transducing membranes (e.g., cytoplasmic membranes of bacteria, thylakoid membranes of chloroplasts, and mitochondrial inner membranes) is pivotal for the survival of unicellular to complex organisms (Valentine and Valentine 2009). Energy balance in living cells is highly dependent on the efficiency of lipid membranes controlling the permeability of ions and optimizing electron transport at the membrane level, which creates proton gradients enabling mechanical energy output in the form of adenosine triphosphate (Daum et al. 2010; Yoshinaga et al. 2016). This process is mediated by modulation of membrane fluidity and viscosity through regulation in the length and saturation levels of fatty acid chains linked to different polar lipids (Sinensky 1974; Valentine and Valentine 2004). The adjustment of membrane lipids (MLs) composition in response to external abiotic stressors was suggested to be universally mediated by membrane homeoviscosity (Sinensky 1974; Cossins and Prosser 1978; Budin

et al. 2018), which assures optimal cellular functions and interlinks lipids with bioenergetics (Valentine and Valentine 2009; Kellermann et al. 2016; Yoshinaga et al. 2016).

Membranes enriched in polyunsaturated fatty acids (PUFAs) are more susceptible to oxidation by reactive oxygen species (ROS), especially free radicals (Greenberg et al. 2008; Yin et al. 2011). If not contained by the cellular antioxidant machinery (e.g., enzymes and carotenoids), ROS can generate lipid radicals, which might propagate ML oxidation (Smith and Murphy 2008; Niki 2009; Yin et al. 2011)—ultimately unbalancing proton gradients thereby disturbing the energy balance of cells. Lipid oxidation resulting in reduced concentrations of PUFA in energy-transducing membranes is suggested to impair distinct biological and ecological processes across all life forms, as shown in the inhibition of plant and algal growth (Falcone et al. 2004; Luo et al. 2014), coral bleaching (Lesser 1997; Tchernov et al. 2004; Weis 2008), and human neurodegenerative diseases (Farooqui et al. 2000; Cutler et al. 2004; Chaves-Filho et al. 2019).

Coral bleaching is characterized by the physiological impairment of symbiosis between cnidarian hosts and their zooxanthellae symbionts (Symbiodiniaceae) and/or by loss of symbionts' photosynthetic pigments (Glynn 1993), potentially triggered by excessive ROS generation in the symbionts and/or the host (Los and Murata 2004). Higher temperatures lead to increased fluidity of highly unsaturated fatty acids of thylakoidal membranes and may cause leakage of high-energy electrons from the water splitting reaction at the photosystem II (PSII) in Symbiodiniaceae (Slavov et al. 2016). This process is suggested to lead to increased production of ROS and cell damage in the symbionts (Lesser 1997, 2006; Goyen et al. 2017). In addition to increased temperatures, excessive light stress can also intensify the production of ROS via generation of singlet oxygen (Pospíšil 2016). Symbiodiniaceae thylakoid membranes are enriched in glycolipids linked to PUFA (Leblond and Chapman 2000). The greater number of double bonds as compared to mono (MUFA) and saturated (SFA) fatty acids in glycolipids significantly increase their susceptibility to ROS (Yin et al. 2011). Several studies have suggested that Symbiodiniaceae thermal tolerance and bleaching susceptibility of their coral hosts are defined by saturation levels of fatty acids contained in the symbiont's thylakoid membranes. Nonetheless, this possible mechanism was inferred from the analysis of bulk fatty acid composition (Tchernov et al. 2004; Bachok et al. 2006; Kneeland et al. 2013) or from a limited number of lipid classes (Tolosa et al. 2011; Imbs and Yakovleva 2012; Rosset et al. 2019; Solomon et al. 2020).

The oxidative stress theory provides a reasonable concept to explain coral bleaching leading to worldwide coral decline (Oakley and Davy 2018). However, currently, a lipid-based molecular explanation of thermal stress leading to thylakoid membrane oxidative damage is still missing. Here, we show a time-dependent cell fitness (evaluated by population density) and a comprehensive untargeted lipidomic analysis of a heat

shock experiment (sudden rise of 12°C for 4 h) with three different species of coral reef symbionts: *Symbiodinium microadriaticum*, *Breviolum minutum*, and *Cladocopium goreaui*. Although studied here in *in vitro* cultures, all three symbionts are commonly associated with coral hosts (Lajeunesse et al. 2018) and, importantly, were reported to display distinct thermal tolerances. Previous studies have suggested *B. minutum* as a thermal sensitive symbiont, whereas *S. microadriaticum* and *C. goreaui* have been deemed, comparatively, more thermal tolerant species (Swain et al. 2017; Lesser 2019). The heat shock experimental design was aimed at investigating the physiological adaptation of symbionts to thermal stress rather than environmental thresholds of temperature, similarly to previous studies using distinct model organisms (Légeret et al. 2016; Higashi and Saito 2019). Our detailed monitoring of lipid molecular species enabled us to identify biomarkers associated with physiological acclimation strategies in response to extreme heat stress in Symbiodiniaceae. In addition to symbionts lipidome, major pigments (carotenoids and chlorophylls) and plastoquinone were also analyzed to evaluate stress response at the membrane level.

Methods

Experimental setup

Symbiodiniaceae monocultures (*S. microadriaticum*—ITS2 A1, ID: CassKB8; *B. minutum*—B1, Ap04 and *C. goreaui*—C1, Mp) were received from the University at Buffalo (New York) and kept in BMAK microalgae facility at the Instituto Oceanográfico from Universidade de São Paulo (Brazil). The cultures of each symbiont were replicated equally into six 1-liter Erlenmeyer bottles (heat shock and control samples were performed in triplicates) containing sterile natural sea water with *f/2* nutrient conditions (Guillard and Ryther 2011). Bottles were randomly distributed in a water bath maintained at 22°C. Sterilized temperature sensors ($\pm 0.5^\circ\text{C}$) were added inside the cultures of each bottle to monitor temperature throughout the experiment. Cool fluorescent lights were used, and light availability kept constant at $80 \mu\text{E m}^{-2} \text{s}^{-1}$ in a 12:12 h light/dark cycle. Initial cell numbers in each bottle was $500 \text{ cells mL}^{-1}$ and population densities were monitored over time using a Neubauer counting chamber. Heat shock was performed once all cultures were in exponential growth (10 d of cultivation). A separate water bath was used and prewarmed to 34°C using electrical aquarium heaters ($\pm 0.5^\circ\text{C}$). Three bottles of each symbiont (nine in total) were transferred from 22°C to the preheated water bath container where a temperature of 34°C was reached after 20 min (T_0). Subsequently, the 34°C heat shock period was applied for 4 h. Samples were immediately taken at the end of heat shock period (T_4) to evaluate short-term lipidome alterations between the heat shock and control populations. Afterward, culture bottles were transferred back to the 22°C water baths. Both groups were sampled again after 240 h (T_{244}) for analyses of long-term lipidome changes. Additional samples were collected from the heat shock populations 1 d after the event (T_{28}) to describe potential rapid recovery of lipidome profiles

after a return to the initial temperature (please see experimental design in Supporting Information Fig. S1). Bottles were slowly hand rotated for homogenization before sampling, which occurred all at the same time during the light phase. Samples for lipid and pigment analysis were taken with sterile pipets and subsequently filtered onto precombusted GF/F filters (10 h under 300°C). Cell numbers exceed 1 million per filter and the true number of cells per filter was then calculated from the cell density in the remainder of the cultures after filtration on the sampling days.

Lipid and pigment standards

Internal standards (IS) for sphingolipids, phospholipids, and storage lipids were obtained from Avanti Polar Lipids. They were added to each sample allowing for further identification and quantitative corrections. Description and concentration of each component are shown in Supplementary Table S8. Aminolipids and glycolipids as well as pigments were quantified using external calibration curves with standards obtained from Avanti Polar Lipids and DHI Labs, respectively.

Lipid extraction

Lipid extraction, including pigments and plastoquinone, was performed according to Yoshida et al. (2008). Each GF/F sample filter was macerated and homogenized in 1 mL of 10 mM phosphate buffer (pH 7.4) containing deferoxamine mesylate 100 μM as chelating agent. Then, 800 μL of methanol and 200 μL of IS mix (10 $\mu\text{g mL}^{-1}$, diluted in methanol:isopropanol [1:1]) were added. Next, 4 mL of chloroform:ethyl acetate (4:1) were added to each mixture and thoroughly vortexed for 1 min. Samples were sonicated for 20 min and all procedures were performed on top of crushed ice to minimize evaporation of the solvents. After centrifugation (2000 $\times g$ for 6 min at 4°C), the lower phase containing the total lipid extract (TLE) was transferred to a new tube and dried under N_2 gas. Dried TLE was again dissolved in 100 μL of isopropanol for analysis and the injection volume was set at 1 μL .

Lipidomic analysis and data processing

TLE was analyzed using an electrospray time-of-flight mass spectrometer (ESI-TOFMS, Triple TOF 6600, Sciex) interfaced with an ultra high-performance LC system (UHPLC Nexera, Shimadzu), as described previously in Chaves-Filho et al. (2019).

MS/MS data were analyzed with PeakView[®] and lipid molecular species were manually identified and annotated. The interpretation of MS/MS spectra, showing fragment ions as well as exact masses and retention times used for identification, is presented in the Supporting Information. Our strategy was to describe the most abundant ions obtained by MS/MS experiments, covering in general more than 80% of the total ion counts. Pigments, plastoquinone, cholesterol, diacylglycerol (DAG), triacylglycerol (TAG), and cholesteryl ester (CE) were analyzed in the positive mode whereas MLs such as aminolipids and glycolipids were identified in the positive mode, but quantified in the negative

mode. All other MLs and free fatty acids (FFA) were analyzed in the negative mode. The peak areas of lipid molecular species were obtained by MS data, within 5 ppm accuracy, from MultiQuant[®]. For quantification, the peak areas of lipid species were divided by the peak areas of their corresponding IS (shown in detail in Supplementary Table S8). Pigments, cholesterol, and FFA had external calibration curves relative to LysoPC (17:0) IS; DAG had external calibration curve relative to TAG (17:0/17:0/17:0) IS. Phosphatidylinositol (PI), aminolipids, and glycolipids had external calibration curves relative to PC (17:0/17:0) IS. They were injected separately following dilution curves with 11 points each based on concentration ranges described in Supplementary Tables S9, S10. Throughout the dilution curves, each point had half the concentration of the previous point and lower limits were defined based on MS inferior limit of detection. Specific correction factors were calculated as slopes from graph curves of each external standard divided by their respective abovementioned IS. For these specific groups, final concentrations were obtained from the peak area ratio divided by their respective IS area ratio and multiplied by their respective correction factor (for details, see Supplementary Tables S9, S10). No external calibration was performed for plastoquinone. Its peak area was divided by the peak area of Lyso PC (17:0) given their similarities in retention time. Therefore, plastoquinone concentrations are not comparable to the other lipid compounds, but they are still largely comparable among samples. During our untargeted analysis, several oxidized PUFA were identified and quantified both as MLs and their FFA forms. The lipidomic analysis, however, did not allow distinguishing the exact position of monohydroxides and hydroperoxides from these oxidized PUFA. For this purpose, we conducted an additional analysis using targeted oxylipidomics to ascertain the composition of specific isomers of oxidized fatty acids (see below).

Oxylipidomic analysis

Different abiotic and biological processes, including singlet oxygen, radical, and enzymatic oxidation generate specific isomers of oxidized fatty acids. To determine the contribution of specific isomers of oxidized fatty acids, a targeted oxylipidomic method was applied to monohydroxides derived from linoleic and docosahexaenoic acids (DHA), respectively, hydroxyoctadecadienoic (HODE) and hydroxydocosahexaenoic (HDoHE) acids available in our laboratory. The HODE and HDoHE standards were synthesized and purified as previously described in Derogis et al. (2013). In brief, TLE was spiked with the deuterated IS 5-hydroxyeicosatetraenoic acid (5-HETE-d8) (100 ng) and 9-hydroxyoctadecadienoic acid (9-HODE-d4) (100 ng) and analyzed using an ESI-TOFMS interfaced with a UHPLC system. Samples were loaded into a BEH column (UPLC[®] C18 column, 1.7 μm , 2.1 mm i.d. \times 100 mm) with a flow rate of 0.5 mL min^{-1} and oven temperature at 35°C. For reverse phase (RP) LC, the mobile phase A consisted of acetic acid:water:acetonitrile (0.02:50:50), while mobile phase B composed of acetic acid:acetonitrile:isopropanol (0.02:50:50) and

lipid analyses were performed in negative ionization mode (Wang et al. 2014). The linear gradient during RP LC was as follows: from 0.1% to 55% B over the first 4 min, 55% to 99% B from 4 to 4.5 min, hold at 99% B from 4.5 to 6.5 min, decreased from 99% to 0.1% B from 6.5 to 7 min, and hold at 0.1% B from 7 to 10 min. The MS operated in negative ionization mode, and the scan range set at a mass-to-charge ratio of 200–1000 Da. Data for lipid molecular species identification and quantification were obtained with a targeted product ion acquisition method. Data acquisition, using Analyst[®] 1.7.1 with an ion spray voltage of -4.5 kV and the cone voltage at -80 V, was performed with a period cycle time of 0.56 s with 100 ms acquisition time for the MS1 scan and 10 ms for the MS/MS scan. The curtain gas was set at 25 psi, nebulizer and heater gases at 50 psi, and interface heater at 500°C. Specific fragments used for each oxidized lipid were manually identified using PeakView[®] and ChemDraw[®] software (Supplementary Table S11), as previously described (Derogis et al. 2013). Identification and quantification were performed by monitoring specific fragments from each analyte using Multiquant[®] software. The area of analytes was obtained by using 5 mDa as the maximum acceptable mass error. The area ratio obtained for lipid molecular species was calculated by dividing the peak area of the lipid by the corresponding IS (Supplementary Table S11). The concentration of lipid species was calculated by applying the area ratio in a calibration curve constructed for each analyte. Data are presented as relative percentages. This analysis was performed separately from lipidomics, so that data generated here are not comparable to relative percentages, neither to abundances of lipid compounds monitored through lipidomics.

Statistical analysis

All lipid compounds described in our work (260 lipid molecules) were sorted into the main lipid classes and subclasses (Supplementary Table S1). Differences among the lipidomes of symbionts growing at 22°C (controls) were established before applying the heat shock considering the total sum of compounds concentrations in each lipid class. For that, we used a one-way ANOVA analysis followed by Tukey's HSD ($p < 0.05$) and false discovery rate correction using MetaboAnalyst 4.0 software (Chong et al. 2019). A two-way analysis of covariance (ANCOVA) was performed to test for significant differences in cell density development over time between the control and heat shock groups of each species. ANCOVA used time (hours of experiment) as a covariable and heat shock ($[T]/\text{control } [C]$) nested within each lipid. Pairwise comparisons between heat shock and control within the same time; and heat shock over time (T_4 , T_{28} , and T_{244}), for each symbiont were tested with Tukey's HSD post hoc test ($p < 0.05$) (JMP v8.0 statistical software).

Overall individual lipid alterations caused by heat shock in each symbiont species were validated by t -test ($p < 0.05$) in pairwise comparisons (heat shock \times control) at T_4 and T_{244} considering changes relative to the total number of lipid molecular species. Further quantitative differences focused on

MLs and pigments exclusively (133 features). First, multi-dimensional scaling (MDS) and analysis of similarity (ANOSIM) (both ran with Primer 6.0; Clarke et al. 2014) were used to visualize and test the differences among heat shock and control in each and among symbiont species. Positive pairwise R values from ANOSIM were used as indicators of the intensity of ML remodeling caused by heat shock in each Symbiodiniaceae. Principal component analysis (PCA) was used to identify the subclasses of MLs responsible for the main differences caused by heat shock. After this screening, each one of these subclasses was tested for significant differences among the experimental units with a three-way mixed ANOVA to evaluate the differences between heat shock and control among symbiont species using heat shock (HS; two levels: control and treatment) orthogonal to time (Ti; two levels: T_4 and T_{244}) and nested within each Symbiodiniaceae species (Spp.; three levels: A1, B1, and C1). A further two-way crossed ANOVA was performed to evaluate the differences between heat shock and control individually in each symbiont species using heat shock (HS; two levels: control and treatment) orthogonal to time (Ti; two levels: T_4 and T_{244}). Pairwise comparisons were tested with Tukey's HSD test, and the significance threshold was set at $p < 0.05$. The same matrix of 133 lipids was used for similarity percentages (SIMPER) analyses (using Primer 6.0) comparing heat shock and control of each symbiont for identification of individual lipid compound as heat stress biomarkers. All data of parametric tests were tested for homoscedasticity and log-transformed when necessary. Data was log-transformed (except in SIMPER analyses), so that the variations in less abundant lipids are comparable to more abundant compounds.

Results

A comprehensive untargeted lipidomic assessment was performed under standard culture conditions (22°C; see the Methods section for details) to establish a baseline for comparing the three Symbiodiniaceae species: *S. microadriaticum* (ITS2 type A1), *B. minutum* (B1), and *C. goreauii* (C1). A total of 260 compounds were identified and sorted into seven classes (i.e., pigments, MLs as glycolipids, aminolipids, phospholipids, and sphingolipids; storage lipids and others) (see Supplementary Table S1 and Supporting Information Fig. S2, data available at doi:10.17632/cpr9skxb4j.1). We have also reported the relative abundance of 16 different isomers of monohydroxy fatty acids (see below). The most significant difference in abundance of lipid classes among the three species was observed in the concentration of MLs (Supplementary Table S2), which was up to 40% lower in *B. minutum* than in the other two species (Fig. 1a). Most of the individual lipid compounds (75 out of 86) that significantly differed among the three species were ML components (Supporting Information Fig. S2). Of these 75 compounds, 43 of them were esterified to omega-3 fatty acids, either octadecatetraenoic acid

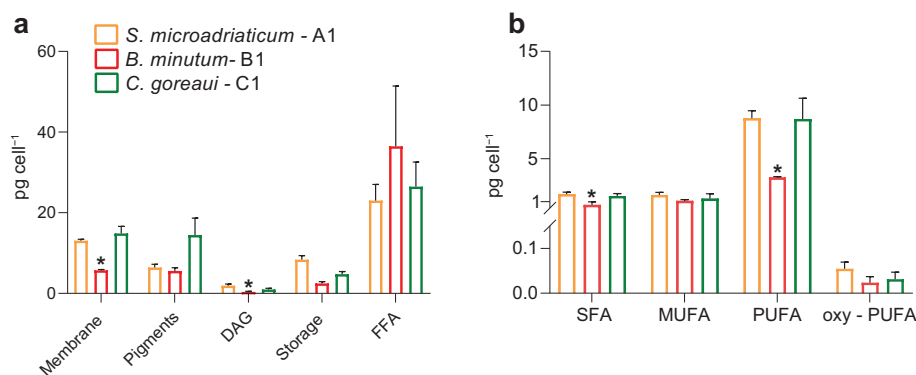


Fig. 1. Main lipid classes characterized in Symbiodiniaceae species and saturation index of their MLs growing at baseline (22°C, controls). Mean abundance and their respective standard error bars for (a) the main lipid classes. MLs encompass glyco-, phospho-, amino-, and sphingo-lipids, plus cardiolipin and cholesterol. Chlorophylls and carotenoids were summed into pigments. TAG and CEs were summed into storage lipids. DAG and FFA were represented separately; (b) summary of SFA, MUFA, PUFA, and oxidized PUFA (oxy-PUFA) esterified to ML. Bars with an asterisk (*) are significantly different ($p < 0.05$) within a given lipid class. Statistical indicators are given in Supplementary Table S2.

(18:4n-3), octadecapentaenoic acid (18:5n-3), or DHA (22:6n-3). Glycolipids were predominantly linked to 18:4 and 18:5, whereas phosphatidylcholine (PC) and 1,2-diacylglyceryl-3-(O-carboxyhydroxymethylcholine) (DGCC) were mostly linked to DHA (Supplementary Table S1). The amounts of membrane-bound oxidized PUFA (oxy-PUFA) did not differ significantly among the three species at baseline (Fig. 1b).

To assess the influence of heat shock on Symbiodiniaceae fitness, both heat shock and control cultures of each symbiont were sampled over time for population density. Biomass sampling for lipidomics was performed immediately after the 4-h-long heat shock (T_4), then a day later (T_{28}), and finally at the end of the experiment of 240 h (T_{244}). Even though the control of *S. microadriaticum* had low population density number at T_{244} , no significant differences among the growing control

cultures of the three species were noticed (Fig. 2). Although the population density number of *C. goreauii* was not significantly reduced by the heat shock, both *S. microadriaticum* and *B. minutum* showed an initial reduction to about half of their population compared to control already at T_4 , resulting in significantly affected growth curves (Fig. 2; Supplementary Table S3). The only symbiont that fully ceased growth was *B. minutum*, indicated by the constant decline in its population density after heat shock (Fig. 2).

Overall alterations in lipidome profiles after heat shock

Qualitative changes in the symbionts' lipidome were examined by *t*-test in pairwise comparisons at 4 (T_4) and 240 h (T_{244}) after heat shock relative to time-matched control samples. Our findings revealed an intense lipidome remodeling

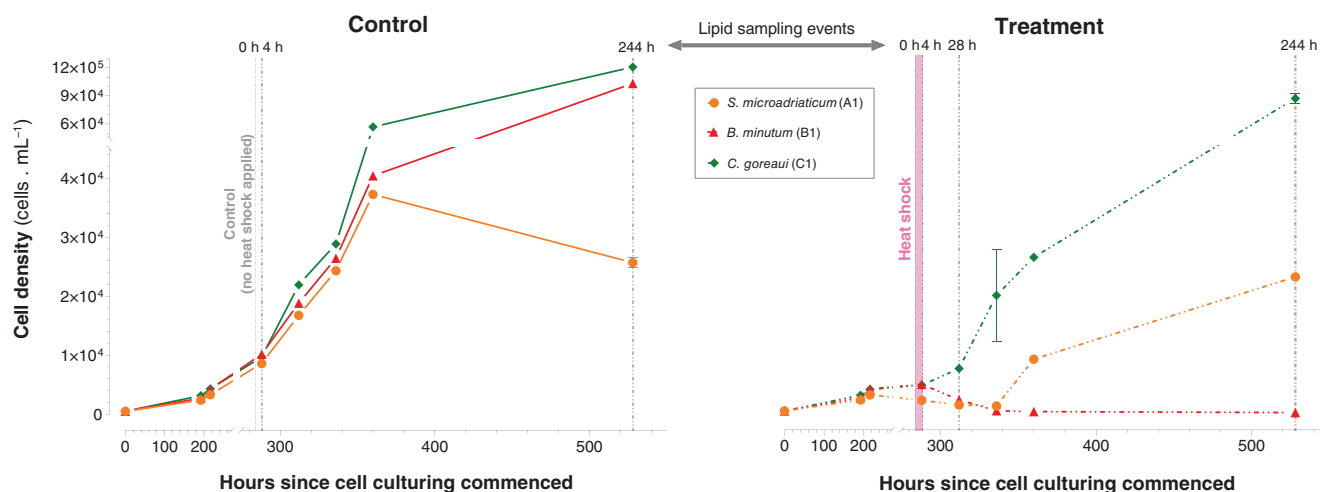


Fig. 2. Variation of Symbiodiniaceae population densities since cell culturing commenced. Controls (left) were cultured at 22°C throughout the experiment. Heat shock treatment samples (right) were exposed to 34°C for 4 h after population densities reached exponential growth and were transferred back to 22°C until the end of the experiment. Break in the x- and y-axes indicates change in scale to highlight population density after the heat shock. Vertical gray lines indicate sampling for lipidomic analysis (i.e., at 0, 4, 24, and 240 h after the heat shock). Cultures were sampled in triplicates and data is represented as average populational density number with standard errors. Statistical indicators are given in Supplementary Table S3.

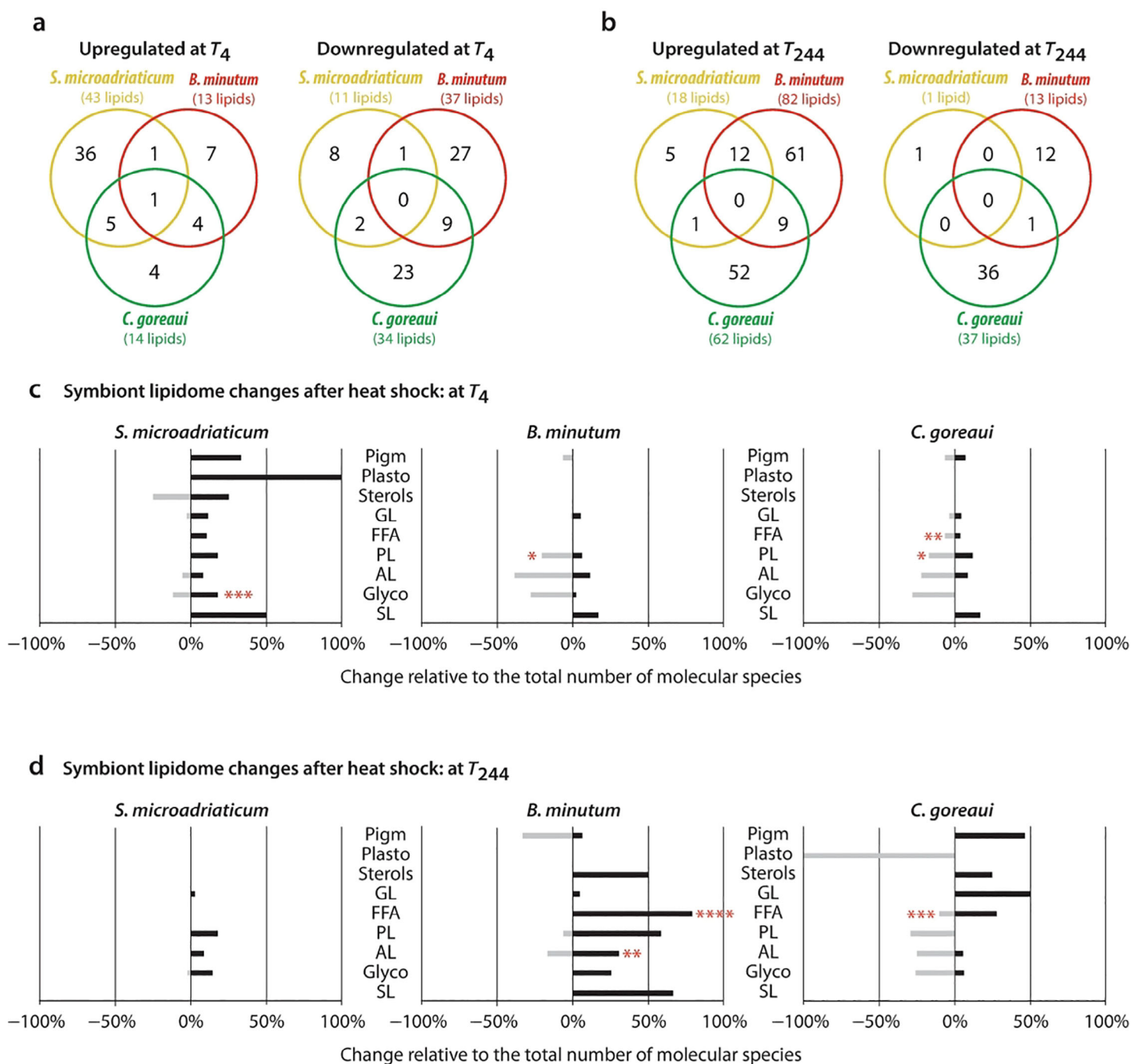


Fig. 3. Qualitative alterations in the number of individual lipids and pigments, and their contribution within subclasses, significantly altered (t -test; $p < 0.05$) in Symbiodiniaceae after heat shock as compared to controls. Venn diagrams displaying the number of compounds significantly up- and down-regulated in pairwise comparisons at 4 (T_4) and 240 h (T_{244}) after heat shock vs. their controls (**a** and **b**, respectively). Contribution of altered individual compounds to the total number of compounds within a subclass (in %) at T_4 and T_{244} vs. their controls (**c** and **d**, respectively). Red star symbols indicate the number of significantly altered oxidized lipids within a given subclass. Analyses details are shown in Supplementary Table S4. Pigments (Pigm), plastoquinone (Plasto), CEs and free cholesterol (Sterols), glycerolipids (GL) represented by TAG and DAG; FFA, phospholipids (PL), aminolipids (AL), glycolipids (Glyco), and sphingolipids (SL).

already at T_4 . All species displayed around 50 significant changes in lipid composition, including up- and down-regulated compounds (Fig. 3a; Supplementary Table S4). At T_{244} , *S. microadriaticum* showed fewer alterations in lipidome

(ca. 20 lipids) as compared to the other two species that presented ca. 100 significantly altered lipids (Fig. 3b; Supplementary Table S4). As shown in the Venn diagrams, only few overlapping alterations in lipidome were observed, suggesting

that changes in lipid and pigment compositions were largely species-specific. Figure 3c,d illustrates the contribution of changes in symbionts' lipidome with respect to the percentage of individual lipids within a subclass. The initial alterations (i.e., 4 h after the heat shock) were associated with decreased concentrations of MLs such as aminolipids and glycolipids as well as an increase in sphingolipids for all three symbiont species (Fig. 3c; Supplementary Table S4). Lipidome alterations at T_{244} revealed different strategies for *B. minutum* and *C. goreau*, the two species displayed around 100 significant changes. In contrast to the upregulation of pigments and glycerolipids, particularly TAG, in *C. goreau*, lipidome changes in *B. minutum* were related to reduced concentrations of pigments, increased concentrations of FFA and MLs, the latter mostly linked to saturated fatty acids (Fig. 3d; Supplementary Table S4). Of note, over 50% of all FFA and sphingolipids exhibited increased concentrations at T_{244} in *B. minutum*. Finally, a number of changes in lipid composition were related to oxidized forms annotated as "red star symbols" in Fig. 3c,d. This finding again suggests species-specific physiological adaptations to heat stress. For instance, whereas the concentrations of oxidized lipids were relatively reduced in *C. goreau*, these bioactive compounds were enriched relative to control samples at T_4 and T_{244} in *S. microadriaticum* and *B. minutum*, respectively.

To evaluate thermal susceptibility (defined by changes in the population densities of each symbiont) together with the

intensity of ML remodeling, both between species and time-dependent variation within species, the MDS plot was applied (Fig. 3a). *B. minutum* greatly changed its membrane lipidome ($R = 0.75$) with no recovery at 24 and 240 h after heat shock (Fig. 4a), which suggests irreversible damaged and/or cell death. *S. microadriaticum* displayed intermediate heat tolerance ($R = 0.73$) and *C. goreau* was the most heat tolerant symbiont ($R = 0.68$). Differences among treatments of both *S. microadriaticum* and *C. goreau* were within 30 Bray-Curtis similarity indices, independent of heat shock treatment at all monitored times. The same similarity was shared only by the control of *B. minutum* (Fig. 4a). Glycolipids, plastoquinone, and pigments, together with cardiolipin, PC, and the total sum of oxy-PUFA esterified to glycolipids and DGCC were the ML classes that exhibited the highest variation among Symbiodiniaceae after heat shock, according to PCA (Fig. 4b). The greater distancing of heat shock-treated samples of *B. minutum* evidenced in both PCA and MDS (i.e., filled red symbols; Fig. 4) also suggests that this heat sensitive symbiont suffered the greatest lipidome alterations.

Quantitative alterations in the heat sensitive symbiont *B. minutum*

The concentration of glycolipids (as the sum of all molecular species from monogalactosyl-diacylglycerol [MGDG] and digalactosyl-diacylglycerol [DGDG]) in *B. minutum* was 77% lower than the controls at T_4 (Fig. 5a). This variation is explained by

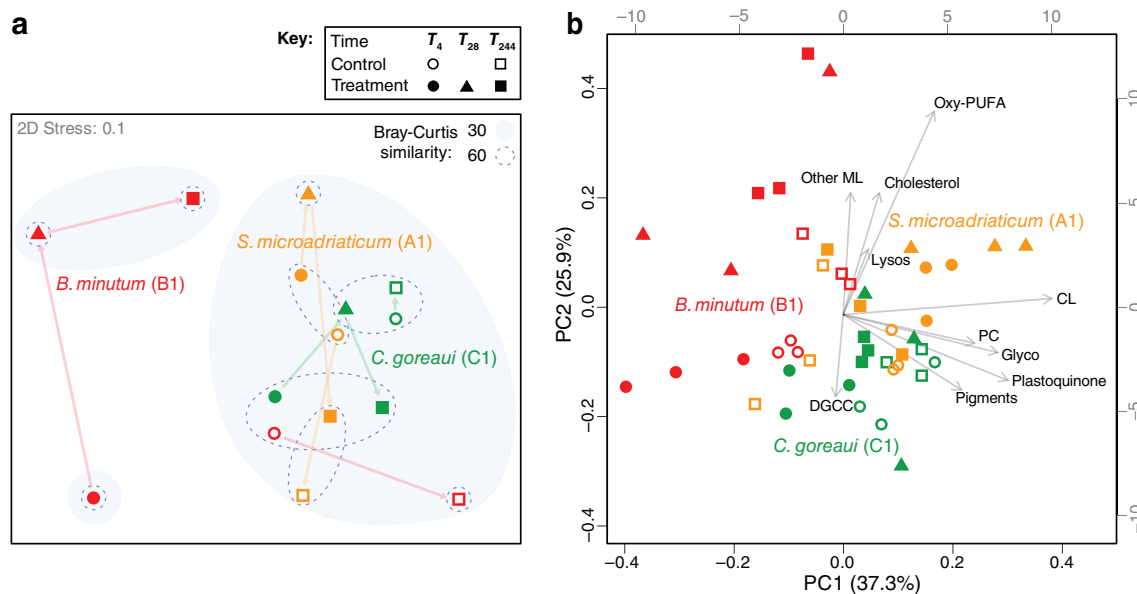


Fig. 4. Remodeling of MLs and pigments in Symbiodiniaceae after heat shock. (a) MDS plot shows averages of the triplicate experiments for each symbiont (*S. microadriaticum*, A1 [yellow]; *B. minutum*, B1 [red]; and *C. goreau*, C1 [green]) at each sampling point for cultures maintained at 22°C (control samples; i.e., T_4 and T_{244}) and exposed to heat shock after 4, 24, and 240 h of treatment (i.e., T_4 , T_{28} , and T_{244}); (b) PCA of ML subclasses, pigments, and plastoquinone of Symbiodiniaceae species. Total concentration of the sum of all lipid compounds constituting each ML subclass (represented in vectors) was used to simplify analysis (cf. Supplementary Table S1). Lipid subclasses that were either more abundant or that had polar head groups esterified to PUFA and/or PUFA derived products were presented as single vectors, whereas others MLs were classified as other ML. CL, cardiolipin; Glyco, glycolipids. Oxidized PUFA esterified to glyco, PC, and DGCC were grouped as oxy-PUFA. Lyso-glycolipids, -PC, and -DGCC were grouped as Lysos. Minor membrane components were grouped as other MLs (detailed in Supplementary Table S1). Carotenoids and chlorophylls, including Chl *a*, were grouped as pigments.

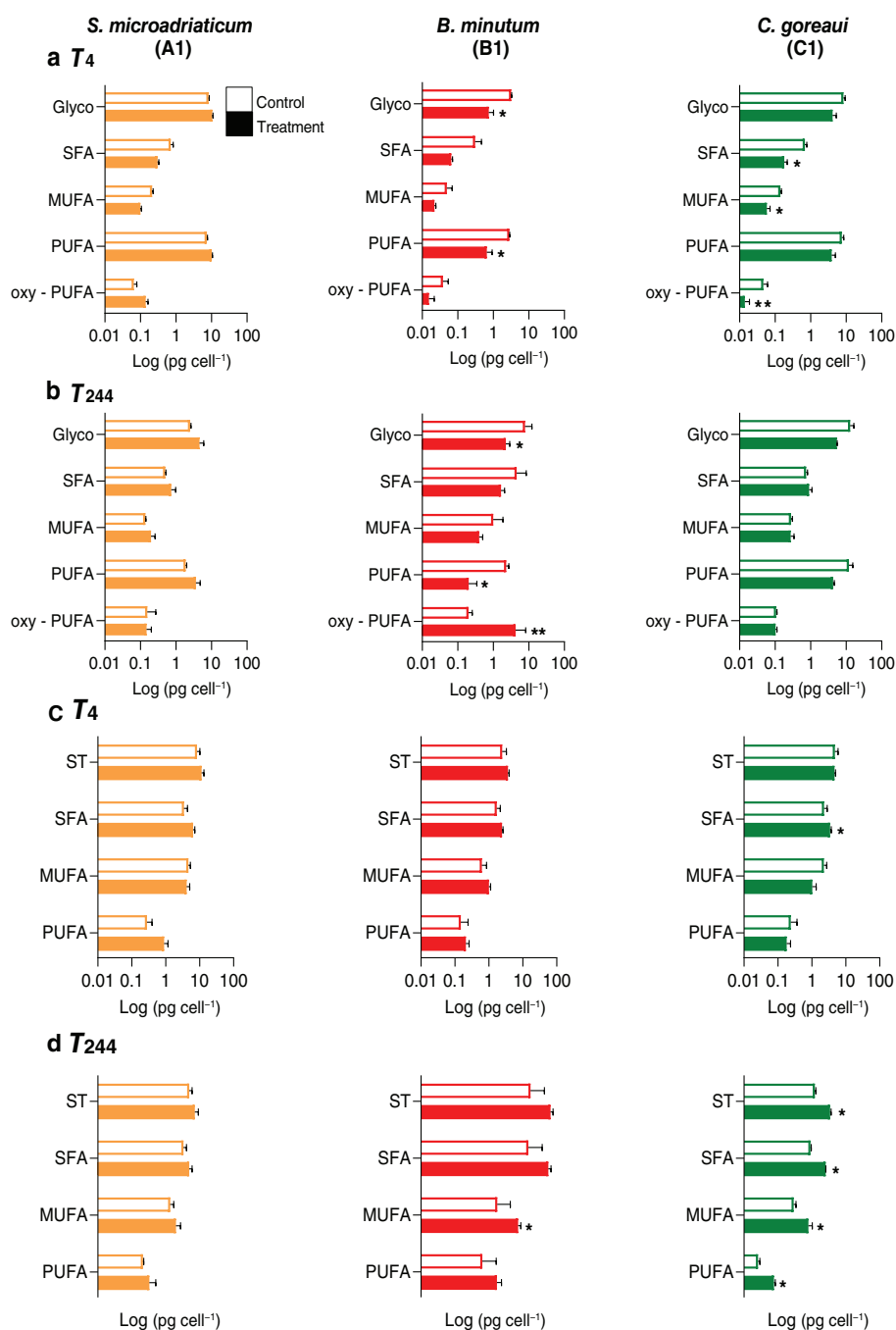


Fig. 5. Quantitative variations in the degree of saturation from glycolipids (essential thylakoid MLs) and storage lipids in Symbiodiniaceae after heat shock. Graphs show mean abundance of both control (empty bars) and heat shock treatment (filled bars) for each Symbiodiniaceae species (*S. microadriaticum*, A1 in yellow; *B. minutum*, B1 in red; and *C. goreau*, C1 in green). Variations of total sums of (a) glycolipids (Glyco) at T_4 (end of heat shock); (b) Glyco at T_{240} (end of experiment); (c) storage lipids (ST) at T_4 ; (d) ST at T_{240} . SFA, MUFA, PUFA, and oxy-PUFA acyl chains linked to glycolipids and storage lipids were normalized in Log_{10} and displayed with their respective standard error bars. Asterisks (* and **) indicate significant pairwise differences (Tukey's HSD, $p < 0.05$) for heat shock [Spp.] and time [Spp.] factors, respectively. Statistical indicators are given in Supplementary Tables S5, S6.

the reduction of PUFA linked to glycolipids (i.e., the sum of all PUFA within this lipid subclass; Fig. 5a,b). At T_{244} , the concentration of PUFA linked to glycolipids was 91% lower, whereas the concentration of oxy-PUFA linked to glycolipids increased by 20 times compared to the control (Fig. 5b). The glycolipid

species MGDG (18:4/18:5-OH) and DGDG (18:4/18:5-OH) were among the top 20 most relevant altered lipids at T_{244} relative to controls (Supplementary Table S7). Their concentrations increased by 1.47 and 1.12 pg, respectively, whereas concentrations of their precursors (MGDG [18:4/18:5] and DGDG

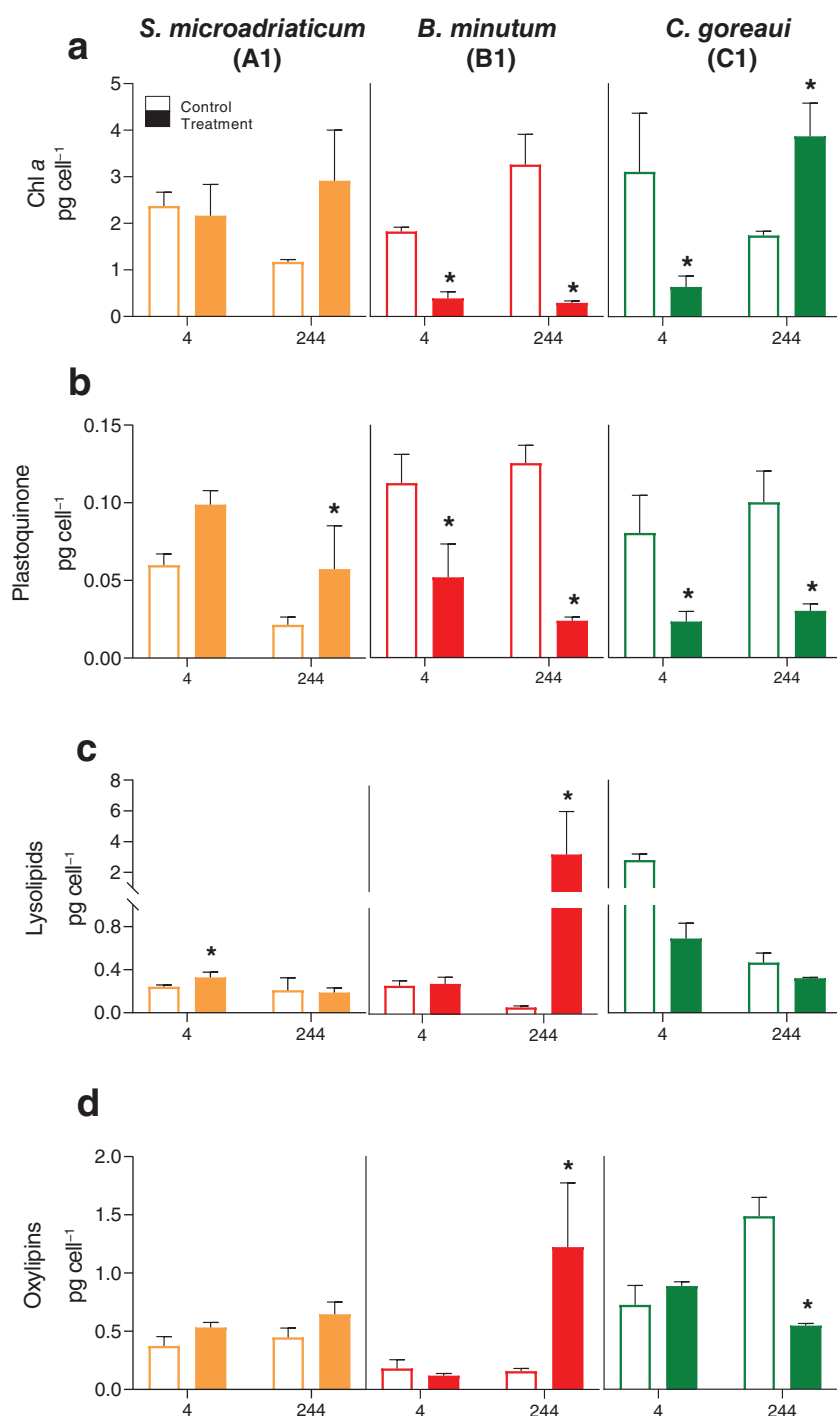


Fig. 6. Quantitative variation of selected compounds in Symbiodiniaceae after heat shock. Mean abundances in pg cell^{-1} and their respective standard error bars of (a) Chl *a*, (b) plastoquinone, (c) lysolipids, and (d) free oxy-PUFA (oxylipins). Graphs show both control (empty bars) and heat shock treatment (filled bars) for each Symbiodiniaceae species (*S. microadriaticum*, A1 in yellow; *B. minutum*, B1 in red; and *C. goreaui*, C1 in green)—at each specific analyzed time T_4 (end of heat shock) and T_{244} (end of experiment). Asterisks (*) indicate significant pairwise differences (Tukey's HSD, $p < 0.05$ for heat shock [Spp.] factor. Statistical indicators are given in Supplementary Table S5.

[18:4/18:5], respectively) dropped to about half at T_4 and did not recover at the end of experiment (Supplementary Table S7). The concentrations of lysolipids and free oxy-PUFA (oxylipins) also increased significantly at T_{244} (Fig. 6c,d). The positional

isomers of monohydroxyoctadienoic (HODE) and monohydroxydocosahexaenoic (HDoHE) acids, derived from linoleic acid (LA; 18:2n-6) and DHA (22:6n-3), respectively, were further investigated by oxylipidomics. The most abundant

LA-derived oxylipins, independent of heat shock exposure, were 9- and 13-HODE isomers (Supporting Information Fig. S5). Relative percentages of 14- and 19-HDoHE isomers were higher than control only at 240 h after heat shock compared to control (Supporting Information Fig. S6). Concentrations of both plastoquinone and chlorophyll (Chl) *a* were reduced after heat shock (Fig. 6a,b), similarly to glycolipids. The concentrations of PC, DGCC, and cholesterol decreased after heat shock, whereas sphingolipids (i.e., the sum of ceramides, phytoceramides, and hexosyl-ceramides) increased, exhibiting a more than fivefold gain at T_{244} (Supporting Information Fig. S4). Overall, the storage lipids did not change significantly after heat shock, but the MUFA content increased in TAG at T_{244} (Fig. 5c,d).

Quantitative alterations in the heat tolerant symbionts

S. microadriaticum and *C. goreau*

In *S. microadriaticum*, the concentrations of Chl *a* and the sum of molecular species in glycolipids, oxylipins, sphingolipids, and storage lipids did not change significantly (Figs. 5, 6a,d, and Supporting Information Fig. S4). Plastoquinone, free cholesterol, and the sum of lysolipids, PC, and DGCC slightly increased at either T_4 or T_{244} or both (Fig. 6b,c and Supporting Information Fig. S4). In *C. goreau*, plastoquinone, PC, and DGCC concentrations decreased similarly (Fig. 6b and Supporting Information Fig. S4), whereas Chl *a* decreased at T_4 , but increased at the end of experiments, compared to control (Fig. 6a). Significant decrease in glycolipids concentration in *C. goreau* at T_{244} was only validated by a two-way ANOVA species-specific analysis (Supplementary Table S6) representing a drop of 35% compared to the control samples (Fig. 5b). The concentration of oxy-PUFA esterified to glycolipids was uniquely lower than control at T_4 in *C. goreau* (Fig. 5a). *C. goreau* also displayed the lowest oxylipins content (among all symbionts), independently of heat shock (Fig. 5a,b). Interestingly, storage lipids concentration increased in *C. goreau* at T_{244} , and the greatest change was observed for PUFA acyl chains esterified to TAG, which were three times greater than the controls (Fig. 5d). Regarding the relative percentages of HODE and HDoHEs isomers, similar contributions were observed after heat shock compared to controls in both heat tolerant symbionts (Supporting Information Figs. S4, S6).

Discussion

An increasing interest in lipid analysis of Symbiodiniaceae has been witnessed over the past two decades (Tchernov et al. 2004; Bachok et al. 2006; Tolosa et al. 2011; Imbs and Yakovleva 2012; Kneeland et al. 2013; Rosset et al. 2019; Solomon et al. 2020; Roach et al. 2021), mainly given the high sensitivity of lipids to thermal alterations and oxidative stress. Here, we applied a comprehensive lipidomic analysis to understand lipidome remodeling of three symbiont species after heat shock. Our data revealed considerable alterations in lipid and pigment compositions at 4 (T_4) and 240 h (T_{244}) after heat shock, with the number of significantly altered

compounds ranging from ca. 20 to 100 relative to control samples (Fig. 3a,b). Lipidome remodeling was largely species-specific and occurred in both heat sensitive (*B. minutum*) and heat tolerant (*S. microadriaticum* and *C. goreau*) species.

The growth arrest in *B. minutum* was initially (already at T_4) linked to reduced concentrations of glycolipids, pigments such as Chl *a* and the PSII electron transporter plastoquinone, suggesting impaired thylakoid membrane function. Subsequently, the data also revealed an increase in the concentration of oxy-PUFA esterified to glycolipids and aminolipids after heat shock, which indicates that a cellular damage caused by heat stress was associated with the oxidation of MLs. In line with this idea and supporting the detoxifying roles of enzymes such as ML-specific lipases (van Kuijk et al. 1987; Miyamoto et al. 2003), the total amounts of lysolipids and free oxylipins were also increased in *B. minutum*, particularly at the end of the experiment when population densities were the lowest (Figs. 6c,d, 2, respectively). Given the steep drop in cell densities already at T_4 and their continued decline toward the end of experiment, we cannot rule out a major event of cellular death during the heat stress incubations with *B. minutum*. Nonetheless, individual compounds from distinct lipid classes displayed increased concentrations at T_{244} (Figs. 3b, 5b,d, 6c, d), suggesting active lipid synthesis by this symbiont.

Despite the distinct lipidome strategies adopted by the heat-tolerant *S. microadriaticum* and *C. goreau*, the protection of their energy-transducing membranes against lipid oxidation may be attributed to efficient antioxidant enzymes (Imlay 2013). *B. minutum* has been shown to have a less efficient enzymatic antioxidant machinery than *S. microadriaticum* and *C. goreau* when exposed to heat stress (McGinty et al. 2012), which is consistent with the considerable reduction in its population density after heat shock. *C. goreau* has been reported to present the highest baseline levels of superoxide dismutase and peroxidases (putative antioxidant enzymes that avoid propagation of superoxide and peroxide ions, respectively) among the three investigated species (Ladner et al. 2012; McGinty et al. 2012; Krueger et al. 2014). This is in line with our findings that revealed *C. goreau* as the most tolerant symbiont (Fig. 2) as well as the one with the lowest concentrations of both, oxy-PUFA esterified to MLs (Fig. 5a,b) and oxylipins (Fig. 6d). Population density of *C. goreau* did not change significantly after heat shock, but the concentrations of most of its MLs (including some glycolipids), chlorophyll, and plastoquinone were reduced when compared to control (Figs. 3, 5 and Supporting Information Fig. S4). In retrospect, lipidome data at T_{244} indicated increased concentrations of storage lipids, especially those linked to PUFA (Fig. 3d, 5d). In *C. goreau*, reallocating PUFA from MLs to TAG or CE (Fig. 5c,d) may represent a strategic mechanism to avoid oxidative stress (Bailey et al. 2015; Chaves-Filho et al. 2019), preserving thylakoid membranes from further damage.

S. microadriaticum has been reported to have lower basal antioxidant enzyme levels than *C. goreau*, although it can boost the production of antioxidant enzymes under stress

(McGinty et al. 2012). Interestingly, an increase in individual compounds of oxidized glycolipids was observed at T_4 (Fig. 3c), whereas at the end of experiment this symbiont displayed the lowest numbers of changes in lipid and pigment compositions (Fig. 3d). Of note, *S. microadriaticum* increased the concentration of some subclasses of MLs after exposure to high temperatures (Fig. 5a,b), particularly at T_4 (Fig. 3c). The synthesis of both antioxidants and MLs is energetically costly and might result in relocation of available energy at the expense of other physiological needs such as growth. Such strategy could explain the large drop in population density of *S. microadriaticum* at T_4 (Fig. 2) and its recover at the end of the experiment, even though with significantly lower cell densities as compared to *C. goreau*. In the case of *C. goreau*, no significant drop in its population was observed, but cells had an intense lipid remodeling (Figs. 3d, 5, 6a,b,d, and Supporting Information Fig. S4a,b), which could have reflected epigenetic adaptation (Duncan et al. 2014; Alves Monteiro et al. 2020). Symbionts with such heat resistant traits or that are capable of rapidly remodel their phenotype in response to stressful conditions are more likely to thrive in future warmer oceans (Bindoff 2019). The efficiency of these phenotypic traits for the metabolic symbiosis within coral hosts remains to be explored and might be crucial to predict the success of coral reefs in warmer oceans.

In a seminal paper, Tchernov et al. (2004) suggested that symbionts with high concentrations of PUFA in thylakoid membranes were more sensitive to heat stress, given the susceptibility of PUFA to oxidative damage. However, our findings suggest that heat tolerance/sensitivity in Symbiodiniaceae may not be defined by membrane saturation at baseline. Recall that the heat sensitive *B. minutum* displayed the lowest contribution of PUFA in ML at baseline, contrasting sharply with the high PUFA content in MLs of heat tolerant symbionts (Fig. 1b). Our data are thus consistent with thermal tolerance being defined by the capacity of symbionts to maintain membrane homeoviscosity particularly at the level of structural MLs (Figs. 5, 6). In energy-transducing membranes, high unsaturation levels in MLs enable fast electron flow thereby leading to high energy production (Valentine and Valentine 2004; Kellermann et al. 2016; Budin et al. 2018). Such efficiency in energy transduction provided by highly unsaturated MLs is, however, only plausible with either an extremely constant environment or a concurrent evolution of powerful antioxidant machinery to preserve membrane PUFA against oxidation (Greenberg et al. 2008; Valentine and Valentine 2009; Imlay 2013). In summary, we suggest that lipidomic analysis of oxidized lipids (both membrane-bound and free derivatives) may pave way to discover novel potential biomarkers for symbiont physiological status, including those mediating coral symbiosis establishment and breakdown. Further studies are nonetheless needed especially regarding the definition of positional isomers. For instance, oxylipins in coral hosts (e.g., eicosanoids, prostaglandins, and aldehydes) have been shown to mediate symbiont–host communication and symbiosis impairment

might represent a final consequence of the accumulation of these signaling molecules in response to stress (Hillyer et al. 2016; Matthews et al. 2017; Roach et al. 2021). In addition to free radicals, enzymes such as lipoxygenases may also generate oxylipins, with a few specific types of positional isomers formed by this pathway. Despite described for phytoplankton (Gerwick 1994; Ruocco et al. 2020; Russo et al. 2020) and macroalgae (Chen et al. 2019), enzymes such as lipoxygenases have never been investigated in Symbiodiniaceae. Nevertheless, the great diversity of isomers detected in the heat shock samples compared to controls (see Supporting Information Figs. S5, S6), without preferential generation of positional isomers, suggests oxidized lipids being generated predominantly by free radicals rather than enzymatically.

Finally, increased concentrations of individual sphingolipids components were observed at T_4 as a common feature of all symbionts (Fig. 3c; Supplementary Table S4). Accumulation of sphingolipids in response to heat stress has been reported across all life forms from unicellular bacteria and yeast to plants and mammals, as a strategy to adjust membrane fluidity and permeability (Sollich et al. 2017; Fabri et al. 2020). Furthermore, cell death through canonical apoptosis, such as proposed for mitochondria under oxidative stress, is known to be linked to the upregulation in sphingolipids such as ceramides (Ariga et al. 1998; Hannun and Obeid 2008). In the marine environment, apoptosis mediated by mitochondrial damage in cnidarian host cells was proposed to result in symbiont–host association impairment and to promote bleaching (Dunn et al. 2012). Interestingly, concentrations of all characterized sphingolipids were increased relative to control samples at the end of the heat shock experiment in *B. minutum* (Figs. 3d, 5d). In contrast, concentrations of sphingolipids in the heat tolerant species displayed no alterations relative to control at T_{244} (Figs. 3d, 5d). Despite our limitation to define whether *B. minutum* underwent significant cell death after heat shock, sphingolipids appear as interesting markers to access heat-associated changes in the physiological status of symbionts.

Our study provides a comprehensive baseline for investigating lipidome alterations of Symbiodiniaceae in response to heat stress, with additional support to the oxidative stress theory of coral bleaching (Lesser 1997, 2006). Novel potential biomarkers that are sensitive to physiological changes of Symbiodiniaceae under thermal stress were revealed, including oxidized lipids and sphingolipids. Even though the experiments have been designed for an acute heat stress during a short period of time, which unlikely reflects environmental conditions, our findings revealed relevant species-specific strategies to cope with thermal stress. Such experimental approach has been previously applied to understand organism's adaptation to thermal stress (Légeret et al. 2016; Higashi and Saito 2019). Nonetheless, whether the adaptations at the membrane levels observed in our study of free-living symbionts would be applicable to the holobiont and/or in the environment remain to be tested. The unbiased, untargeted lipidomic approach was pivotal to describe 260 major

compounds comprising symbionts' lipidome and pigments as well as to monitor their fine regulation after heat shock. This study thus also highlights the importance of lipidomics for omics-based systems biology studies aimed to mechanistically understand coral bleaching, which perhaps will contribute to improved strategies for reef conservation in warmer future oceans.

Data availability statement

The data supporting the findings of this study are openly available from Mendeley Database doi:10.17632/cpr9skxb4j.1. Data analyses are provided on Supplementary Tables S2–S7. Additional information about lipidomics and oxylipidomics analyses is available on Supplementary Tables S8–S11.

References

- Alves Monteiro, H. J., C. Brahmī, A. B. Mayfield, J. Vidal-Dupiol, B. Lapeyre, and J. Le Luyer. 2020. Molecular mechanisms of acclimation to long-term elevated temperature exposure in marine symbioses. *Global Change Biology* **26**: 1271–1284. doi:10.1111/gcb.14907
- Ariga, T., W. D. Jarvis, and R. K. Yu. 1998. Role of sphingolipid-mediated cell death in neurodegenerative diseases. *J. Lipid Res.* **39**: 1–16. doi:10.1016/S0022-2275(20)34198-5
- Bachok, Z., P. Mfilinge, and M. Tsuchiya. 2006. Characterization of fatty acid composition in healthy and bleached corals from Okinawa, Japan. *Coral Reefs* **25**: 545–554. doi:10.1007/s00338-006-0130-9
- Bailey, A. P., G. Koster, C. Guillemier, E. M. A. Hirst, J. I. MacRae, C. P. Lechene, A. D. Postle, and A. P. Gould. 2015. Antioxidant role for lipid droplets in a stem cell niche of *Drosophila*. *Cell* **163**: 340–353. doi:10.1016/j.cell.2015.09.020
- Bindoff, N. L. 2019. Changing ocean, marine ecosystems, and dependent communities - research collection. *IPCC special report on the ocean and cryosphere in a changing climate*. 477–587.
- Budin, I., T. de Rond, Y. Chen, L. J. G. Chan, C. J. Petzold, and J. D. Keasling. 2018. Viscous control of cellular respiration by membrane lipid composition. *Science* **362**: 1186–1189.
- Chaves-Filho, A. B., and others. 2019. Alterations in lipid metabolism of spinal cord linked to amyotrophic lateral sclerosis. *Sci. Rep.* **9**: 11642. doi:10.1038/s41598-019-48059-7
- Chen, H., R. Yang, J. Chen, Q. Luo, X. Cui, X. Yan, and W. H. Gerwick. 2019. 1-Octen-3-ol, a self-stimulating oxylipin messenger, can prime and induce defense of marine alga. *BMC Plant Biol.* **19**: 1–16. doi:10.1186/s12870-019-1642-0
- Chong, J., D. S. Wishart, and J. Xia. 2019. Using MetaBoAnalyst 4.0 for comprehensive and integrative metabolomics data analysis. *Curr. Protoc. Bioinform.* **68**: e86. doi:10.1002/cpbi.86
- Cossins, A. R., and C. L. Prosser. 1978. Evolutionary adaptation of membranes to temperature. *Proc. Natl. Acad. Sci.* **75**: 2040–2043. doi:10.1073/pnas.75.4.2040
- Clarke, L. J., J. Soubrier, L. S. Weyrich, and A. Cooper. 2014. Environmental metabarcodes for insects: In silico PCR reveals potential for taxonomic bias. *Mol. Ecol. Resour.* **14**: 1160–1170. doi:10.1111/1755-0998.12265
- Cutler, R. G., J. Kelly, K. Storie, W. A. Pedersen, A. Tammara, K. Hatanpaa, J. C. Troncoso, and M. P. Mattson. 2004. Involvement of oxidative stress-induced abnormalities in ceramide and cholesterol metabolism in brain aging and Alzheimer's disease. *Proc. Natl. Acad. Sci.* **101**: 2070–2075. doi:10.1073/pnas.0305799101
- Daum, B., D. Nicastro, J. Austin, J. R. McIntosh, and W. Kühlbrandt. 2010. Arrangement of photosystem II and ATP synthase in chloroplast membranes of spinach and pea. *Plant Cell* **22**: 1299–1312. doi:10.1105/tpc.109.071431
- Derogis, P. B. M. C., and others. 2013. The development of a specific and sensitive LC-MS-based method for the detection and quantification of hydroperoxy- and hydroxydocosahexaenoic acids as a tool for lipidomic analysis. *PLoS One* **8**: e77561. doi:10.1371/journal.pone.0077561
- Duncan, E. J., P. D. Gluckman, and P. K. Dearden. 2014. Epigenetics, plasticity, and evolution: How do we link epigenetic change to phenotype? *J. Exp. Zool. B: Mol. Dev. Evol.* **322**: 208–220. doi:10.1002/jez.b.22571
- Dunn, S. R., M. Pernice, K. Green, O. Hoegh-Guldberg, and S. G. Dove. 2012. Thermal stress promotes host mitochondrial degradation in symbiotic cnidarians: Are the batteries of the reef going to run out? *PLoS One* **7**: e39024. doi:10.1371/journal.pone.0039024
- Fabri, J. H. T. M., N. P. de Sá, I. Malavazi, and M. Del Poeta. 2020. The dynamics and role of sphingolipids in eukaryotic organisms upon thermal adaptation. *Prog. Lipid Res.* **80**: 101063. doi:10.1016/j.plipres.2020.101063
- Falcone, D. L., J. P. Ogas, and C. L. Sommerville. 2004. Regulation of membrane fatty acid composition by temperature in mutants of *Arabidopsis* with alterations in membrane lipid composition. *BMC Plant Biol.* **4**: 1–15. doi:10.1186/1471-2229-4-17
- Farooqui, A. A., L. A. Horrocks, and T. Farooqui. 2000. Glycerophospholipids in brain: Their metabolism, incorporation into membranes, functions, and involvement in neurological disorders. *Chem. Phys. Lipids* **106**: 1–29. doi:10.1016/S0009-3084(00)00128-6
- Gerwick, W. H. 1994. Structure and biosynthesis of marine algal oxylipins. *Biochim. Biophys. Acta Lipids Lipid Metab.* **1211**: 243–255. doi:10.1016/0005-2760(94)90147-3
- Glynn, P. W. 1993. Coral reef bleaching: Ecological perspectives. *Coral Reefs* **12**: 1–17. doi:10.1007/BF00303779
- Goyen, S., M. Pernice, M. Szabó, M. E. Warner, P. J. Ralph, and D. J. Suggett. 2017. A molecular physiology basis for functional diversity of hydrogen peroxide production amongst *Symbiodinium* spp. (Dinophyceae). *Mar. Biol.* **164**: 46. doi:10.1007/s00227-017-3073-5

- Greenberg, M. E., X.-M. Li, B. G. Gugiu, X. Gu, J. Qin, R. G. Salomon, and S. L. Hazen. 2008. The lipid whisker model of the structure of oxidized cell membranes. *J. Biol. Chem.* **283**: 2385–2396. doi:[10.1074/jbc.M707348200](https://doi.org/10.1074/jbc.M707348200)
- Guillard, R. R. L., and J. H. Ryther. 2011. Studies of marine planktonic diatoms: i. *Cyclotella nana* hustedt, and *Detonula confervacea* (cleve) gran. *Can. J. Microbiol.* **8**: 229–239. doi:[10.1139/m62-029](https://doi.org/10.1139/m62-029)
- Hannun, Y. A., and L. M. Obeid. 2008. Principles of bioactive lipid signalling: Lessons from sphingolipids. *Nat. Rev. Mol. Cell Biol.* **9**: 139–150. doi:[10.1038/nrm2329](https://doi.org/10.1038/nrm2329)
- Higashi, Y., and K. Saito. 2019. Lipidomic studies of membrane glycerolipids in plant leaves under heat stress. *Prog. Lipid Res.* **75**: 100990. doi:[10.1016/j.plipres.2019.100990](https://doi.org/10.1016/j.plipres.2019.100990)
- Hillyer, K. E., S. Tumanov, S. Villas-Bôas, and S. K. Davy. 2016. Metabolite profiling of symbiont and host during thermal stress and bleaching in a model cnidarian–dinoflagellate symbiosis. *J. Exp. Biol.* **219**: 516–527. doi:[10.1242/jeb.128660](https://doi.org/10.1242/jeb.128660)
- Imbs, A. B., and I. M. Yakovleva. 2012. Dynamics of lipid and fatty acid composition of shallow-water corals under thermal stress: An experimental approach. *Coral Reefs* **31**: 41–53. doi:[10.1007/s00338-011-0817-4](https://doi.org/10.1007/s00338-011-0817-4)
- Imlay, J. A. 2013. The molecular mechanisms and physiological consequences of oxidative stress: Lessons from a model bacterium. *Nat. Rev. Microbiol.* **11**: 443–454. doi:[10.1038/nrmicro3032](https://doi.org/10.1038/nrmicro3032)
- Kellermann, M. Y., M. Y. Yoshinaga, R. C. Valentine, L. Wörmer, and D. L. Valentine. 2016. Important roles for membrane lipids in haloarchaeal bioenergetics. *Biochim. Biophys. Acta Biomembr.* **1858**: 2940–2956. doi:[10.1016/j.bbamem.2016.08.010](https://doi.org/10.1016/j.bbamem.2016.08.010)
- Kneeland, J., K. Huguen, J. Cervino, B. Hauff, and T. Eglinton. 2013. Lipid biomarkers in Symbiodinium dinoflagellates: New indicators of thermal stress. *Coral Reefs* **32**: 923–934. doi:[10.1007/s00338-013-1076-3](https://doi.org/10.1007/s00338-013-1076-3)
- Krueger, T., S. Becker, S. Pontasch, S. Dove, O. Hoegh-Guldberg, W. Leggat, P. L. Fisher, and S. K. Davy. 2014. Antioxidant plasticity and thermal sensitivity in four types of *Symbiodinium* sp. (S Lin, Ed.). *J. Phycol.* **50**: 1035–1047. doi:[10.1111/jpy.12232](https://doi.org/10.1111/jpy.12232)
- Ladner, J. T., D. J. Barshis, and S. R. Palumbi. 2012. Protein evolution in two co-occurring types of Symbiodinium: An exploration into the genetic basis of thermal tolerance in Symbiodinium clade D. *BMC Evol. Biol.* **12**: 217. doi:[10.1186/1471-2148-12-217](https://doi.org/10.1186/1471-2148-12-217)
- LaJeunesse, T. C., J. E. Parkinson, P. W. Gabrielson, H. J. Jeong, J. D. Reimer, C. R. Voolstra, and S. R. Santos. 2018. Systematic revision of Symbiodiniaceae highlights the antiquity and diversity of coral endosymbionts. *Curr. Biol.* **28**: 2570–2580. doi:[10.1016/j.cub.2018.07.008](https://doi.org/10.1016/j.cub.2018.07.008)
- Leblond, J. D., and P. J. Chapman. 2000. Lipid class distribution of highly unsaturated long chain fatty acids in marine dinoflagellates. *J. Phycol.* **36**: 1103–1108. doi:[10.1046/j.1529-8817.2000.00018.x](https://doi.org/10.1046/j.1529-8817.2000.00018.x)
- Légeret, B., M. Schulz-Raffelt, H. M. Nguyen, P. Auroy, F. Beisson, G. Peltier, G. Blanc, and Y. Li-Beisson. 2016. Lipidomic and transcriptomic analyses of *Chlamydomonas reinhardtii* under heat stress unveil a direct route for the conversion of membrane lipids into storage lipids. *Plant Cell Env* **39**: 834–847. doi:[10.1111/pce.12656](https://doi.org/10.1111/pce.12656)
- Lesser, M. P. 1997. Oxidative stress causes coral bleaching during exposure to elevated temperatures. *Coral Reefs* **16**: 187–192. doi:[10.1007/s003380050073](https://doi.org/10.1007/s003380050073)
- Lesser, M. P. 2006. Oxidative stress in marine environments: Biochemistry and physiological ecology. *Ann. Rev. Physiol.* **68**: 253–278. doi:[10.1146/annurev.physiol.68.040104.110001](https://doi.org/10.1146/annurev.physiol.68.040104.110001)
- Lesser, M. P. 2019. Phylogenetic signature of light and thermal stress for the endosymbiotic dinoflagellates of corals (family Symbiodiniaceae). *Limnol. Oceanogr.* **64**: 1852–1863. doi:[10.1002/lno.11155](https://doi.org/10.1002/lno.11155)
- Los, D. A., and N. Murata. 2004. Membrane fluidity and its roles in the perception of environmental signals. *Biochim. Biophys. Acta Biomembr.* **1666**: 142–157. doi:[10.1016/j.bbamem.2004.08.002](https://doi.org/10.1016/j.bbamem.2004.08.002)
- Luo, Q., Z. Zhu, Z. Zhu, R. Yang, F. Qian, H. Chen, and X. Yan. 2014. Different responses to heat shock stress revealed heteromorphic adaptation strategy of *Pyropia haitanensis* (Bangiales, Rhodophyta) (S Cotterill, Ed.). *PLoS One* **9**: e94354. doi:[10.1371/journal.pone.0094354](https://doi.org/10.1371/journal.pone.0094354)
- Matthews, J. L., and others. 2017. Optimal nutrient exchange and immune responses operate in partner specificity in the cnidarian–dinoflagellate symbiosis. *Proc. Natl. Acad. Sci.* **114**: 13194–13199. doi:[10.1073/pnas.1710733114](https://doi.org/10.1073/pnas.1710733114)
- McGinty, E. S., J. Pieczonka, and L. D. Mydlarz. 2012. Variations in reactive oxygen release and antioxidant activity in multiple Symbiodinium types in response to elevated temperature. *Microb. Ecol.* **64**: 1000–1007. doi:[10.1007/s00248-012-0085-z](https://doi.org/10.1007/s00248-012-0085-z)
- Miyamoto, S., C. Dupas, K. Murota, and J. Terao. 2003. Phospholipid hydroperoxides are detoxified by phospholipase A 2 and GSH peroxidase in rat gastric mucosa. *Lipids* **38**: 641–649. doi:[10.1007/s11745-003-1109-6](https://doi.org/10.1007/s11745-003-1109-6)
- Niki, E. 2009. Lipid peroxidation: Physiological levels and dual biological effects. *Free Radic. Biol. Med.* **47**: 469–484. doi:[10.1016/j.freeradbiomed.2009.05.032](https://doi.org/10.1016/j.freeradbiomed.2009.05.032)
- Oakley CA, Davy SK. 2018. Cell biology of coral bleaching. Springer. https://link.springer.com/chapter/10.1007/978-3-319-75393-5_8
- Pospíšil, P. 2016. Production of reactive oxygen species by photosystem II as a response to light and temperature stress. *Front. Plant Sci.* **7**: 1950. doi:[10.3389/fpls.2016.01950](https://doi.org/10.3389/fpls.2016.01950)
- Roach, T. N., J. Dilworth, A. D. Jones, R. A. Quinn, and C. Drury. 2021. Metabolomic signatures of coral bleaching history. *Nat. Ecol. Evol.* **5**: 495–503. doi:[10.1038/s41559-020-01388-7](https://doi.org/10.1038/s41559-020-01388-7)
- Rosset, S., G. Koster, J. Brandsma, A. N. Hunt, A. D. Postle, and C. D'Angelo. 2019. Lipidome analysis of Symbiodiniaceae reveals possible mechanisms of heat stress tolerance in reef

- coral symbionts. *Coral Reefs* **38**: 1241–1253. doi:[10.1007/s00338-019-01865-x](https://doi.org/10.1007/s00338-019-01865-x)
- Ruocco, N., and others. 2020. Lipoxygenase pathways in diatoms: Occurrence and correlation with grazer toxicity in four benthic species. *Mar. Drugs* **18**: 66. doi:[10.3390/md18010066](https://doi.org/10.3390/md18010066)
- Russo, E., and others. 2020. Density-dependent oxylipin production in natural diatom communities: Possible implications for plankton dynamics. *ISME J.* **14**: 164–177. doi:[10.1038/s41396-019-0518-5](https://doi.org/10.1038/s41396-019-0518-5)
- Sinensky, M. 1974. Homeoviscous adaptation—a homeostatic process that regulates the viscosity of membrane lipids in *Escherichia coli*. *Proc. Natl. Acad. Sci.* **71**: 522–525. doi:[10.1073/pnas.71.2.522](https://doi.org/10.1073/pnas.71.2.522)
- Slavov, C., V. Schrameyer, M. Reus, P. J. Ralph, R. Hill, C. Büchel, A. W. D. Larkum, and A. R. Holzwarth. 2016. “Super-quenching” state protects Symbiodinium from thermal stress — implications for coral bleaching. *Biochim. Biophys. Acta Bioenerg.* **1857**: 840–847. doi:[10.1016/j.bbabi.2016.02.002](https://doi.org/10.1016/j.bbabi.2016.02.002)
- Smith, W. L., and R. C. Murphy. 2008. Oxidized lipids formed non-enzymatically by reactive oxygen species. *J. Biol. Chem.* **283**: 15513–15514. doi:[10.1074/jbc.R800006200](https://doi.org/10.1074/jbc.R800006200)
- Sollich, M., M. Y. Yoshinaga, S. Häusler, R. E. Price, K. U. Hinrichs, and S. I. Bühring. 2017. Heat stress dictates microbial lipid composition along a thermal gradient in marine sediments. *Front. Microbiol.* **8**: 1550. doi:[10.3389/fmicb.2017.01550](https://doi.org/10.3389/fmicb.2017.01550)
- Solomon, S. L., A. G. Grottoli, M. E. Warner, S. Levas, V. Schoepf, and A. Muñoz-Garcia. 2020. Lipid class composition of annually bleached Caribbean corals. *Mar. Biol.* **167**: 7. doi:[10.1007/s00227-019-3616-z](https://doi.org/10.1007/s00227-019-3616-z)
- Swain, T. D., J. Chandler, V. Backman, and L. Marcelino. 2017. Consensus thermotolerance ranking for 110 Symbiodinium phylotypes: An exemplar utilization of a novel iterative partial-rank aggregation tool with broad application potential. *Funct. Ecol.* **31**: 172–183. doi:[10.1111/1365-2435.12694](https://doi.org/10.1111/1365-2435.12694)
- Tchernov, D., M. Y. Gorbunov, C. de Vargas, S. Narayan Yadav, A. J. Milligan, M. Haggblom, and P. G. Falkowski. 2004. Membrane lipids of symbiotic algae are diagnostic of sensitivity to thermal bleaching in corals. *Proc. Natl. Acad. Sci.* **101**: 13531–13535. doi:[10.1073/pnas.0402907101](https://doi.org/10.1073/pnas.0402907101)
- Tolosa, I., C. Treignier, R. Grover, and C. Ferrier-Pagès. 2011. Impact of feeding and short-term temperature stress on the content and isotopic signature of fatty acids, sterols, and alcohols in the scleractinian coral *Turbinaria reniformis*. *Coral Reefs* **30**: 763–774. doi:[10.1007/s00338-011-0753-3](https://doi.org/10.1007/s00338-011-0753-3)
- Valentine, R. C., and D. L. Valentine. 2004. Omega-3 fatty acids in cellular membranes: A unified concept. *Prog. Lipid Res.* **43**: 383–402. doi:[10.1016/j.plipres.2004.05.004](https://doi.org/10.1016/j.plipres.2004.05.004)
- Valentine, R. C., and D. L. Valentine. 2009. Omega-3 fatty acids and the DHA principle, 1st ed. CRC Press.
- van Kuijk, F. J., A. Sevanian, G. J. Handelman, and E. A. Dratz. 1987. A new role for phospholipase A2: Protection of membranes from lipid peroxidation damage. *Trends Biochem. Sci.* **12**: 31–34. doi:[10.1016/0968-0004\(87\)90014-4](https://doi.org/10.1016/0968-0004(87)90014-4)
- Wang, Y., A. M. Armando, O. Quehenberger, C. Yan, and E. A. Dennis. 2014. Comprehensive ultra-performance liquid chromatographic separation and mass spectrometric analysis of eicosanoid metabolites in human samples. *J. Chromatogr. A* **1359**: 60–69. doi:[10.1016/j.chroma.2014.07.006](https://doi.org/10.1016/j.chroma.2014.07.006)
- Weis, V. M. 2008. Cellular mechanisms of Cnidarian bleaching: Stress causes the collapse of symbiosis. *J. Exp. Biol.* **211**: 3059–3066. doi:[10.1242/jeb.009597](https://doi.org/10.1242/jeb.009597)
- Yin, H., L. Xu, and N. A. Porter. 2011. Free radical lipid peroxidation: Mechanisms and analysis. *Chem. Rev.* **111**: 5944–5972. doi:[10.1021/cr200084z](https://doi.org/10.1021/cr200084z)
- Yoshida, Y., S. Kodai, S. Takemura, Y. Minamiyama, and E. Niki. 2008. Simultaneous measurement of F2-isoprostane, hydroxyoctadecadienoic acid, hydroxyeicosatetraenoic acid, and hydroxycholesterols from physiological samples. *Anal. Biochem.* **379**: 105–115. doi:[10.1016/j.ab.2008.04.028](https://doi.org/10.1016/j.ab.2008.04.028)
- Yoshinaga, M. Y., M. Y. Kellermann, D. L. Valentine, and R. C. Valentine. 2016. Phospholipids and glycolipids mediate proton containment and circulation along the surface of energy-transducing membranes. *Prog. Lipid Res.* **64**: 1–15. doi:[10.1016/j.plipres.2016.07.001](https://doi.org/10.1016/j.plipres.2016.07.001)

Acknowledgments

We thank Linda Waters (Instituto Oceanográfico, University of São Paulo, Brazil), David Valentine (University of California Santa Barbara, USA), Simon Davy (Victoria University of Wellington, New Zealand), and Miguel Mies (Instituto Coral Vivo, Brazil) for reviewing the manuscript. We are also thankful to Florence Schubotz (University of Bremen, Germany) and Frederico Brandini (Instituto Oceanográfico, University of São Paulo, Brazil) for providing standards used in external calibration curves. We are also thankful to the anonymous reviewers for their invaluable comments. This manuscript is a contribution from the Membrane Lipid Code Cracking Society (<http://mlccs.jimdo.com>) and Biological Semiconductor Technologies (<https://www.biologicalsemiconductor.com/>). This study was supported by the Coordenação de Aperfeiçoamento de Pessoal de Nível Superior – Brazil (CAPES) Finance Code 001. Fellowships were received from CAPES to MYY and Fundação de Apoio a Pesquisa do Estado de São Paulo (FAPESP) to A.B.C.-F. and A.I. S.M. was supported by FAPESP (13/07937-8) and Conselho Nacional de Desenvolvimento Científico e Tecnológico (424094/2016-9 and 309083/2017-6). Open access publishing facilitated by Victoria University of Wellington, as part of the Wiley - Victoria University of Wellington agreement via the Council of Australian University Librarians.

Conflict of Interest

None declared.

Submitted 31 January 2022

Revised 06 April 2022

Accepted 16 April 2022

Associate editor: David M. Baker